FORCE-FREE MAGNETIC FIELDS: ERRATA AND ADDITIONS AS OF 2026

Errata

p. 32. In Fig. 3.2, the expression for ψ should be $\psi = r\sqrt{\pi/2r}\, j_{n+\frac{1}{2}}(r)$. This changes the height and width of the figures very slightly.

p. 73. In the paragraph after Eq. (4.33), 4th line, the equation referred to should be Eq. (4.32).

p. 74. First full paragraph, Reference number to Hu should be 25.

p. 77. In the last line before Fig. 4.15, the σ should be a γ.

p. 94. In the last paragraph, line 4, the *S* should be a Σ.

To bring the book up to date, the following additions should be inserted.

ADDITION 1

p. 43. Just after Eq. (3.136) add the following from my paper *A Force-Free Magnetic Field Solution in Toroidal Coordinates*, *Physics of Plasmas* (DOI: 10.1063/5.0146040, 2023).

Introduction

In topology, a torus is a surface of genus one, meaning it has one hole, and the relevant question here is whether it is possible for the surface of a torus to have on it a non-singular force-free magnetic field, meaning one that does not vanish at any point on the surface. Such a field satisfies the force-free magnetic field equation $\nabla \times \boldsymbol{B} = \alpha \boldsymbol{B}$. Arnold [1] has shown that for force-free magnetic fields the field lines will lie on tori provided the field is non-singular and α is not constant. In addition, a theorem by Hopf tells us that that the torus and the Klein bottle are the only smooth, compact, connected surfaces without boundary allowing a vector field without a singularity [2].

It is worth stating the Poincare-Hopf theorem somewhat more formally: If a smooth, compact, connected surface *S* has on it a vector field with only isolated zeros, then its Euler characteristic $\chi(S)$ is an appropriate sum of the index of each zero. Any closed orientable surface is topologically equivalent to a sphere with *p*-handles and Euler characteristic $\chi(S) = 2 - 2p$.

What the Poincare-Hopf theorem states is that only surfaces with Euler Characteristic zero can have a vector field which is nowhere zero. Only the torus and Klein bottle have Euler characteristic zero. Since real Klein bottles in 3-dimensional space cannot exist, only the torus is relevant.

Below it will be shown that there is a non-singular force-free magnetic field restricted to the surface of a torus, and under a restriction on the form of the field, to the interior as well.

Toroidal Coordinates and the Force-Free Relations

Solving for an exact solution to the force-free magnetic field equations in toroidal coordinates is a difficult problem. An extensive history and the approaches used to solve both the exterior and interior toroidal problem has been given by Marsh [3]. In particular, for the interior problem no exact solution is known and one obtains a first order differential equation for α, which can most likely only be dealt with by numerical methods.

There are numerous definitions for toroidal coordinates, and the one used here is shown in Fig. 1

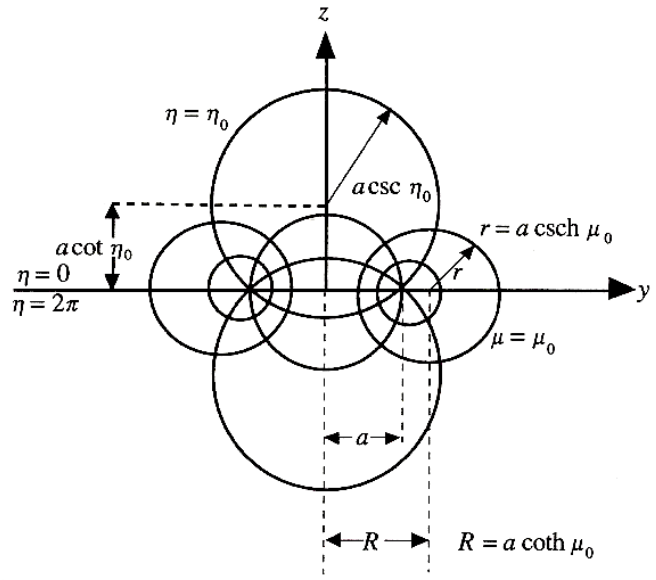

Figure 1. Toroidal coordinates. Note that $a^2 = R^2 - r^2$.

The relation between rectangular coordinates and toroidal coordinates is given by

$$x = \frac{a\,\sinh\mu\,\cos\phi}{\cosh\mu - \cos\eta}, \quad y = \frac{a\,\sinh\mu\,\sin\phi}{\cosh\mu - \cos\eta} \quad z = \frac{a\,\sin\eta}{\cosh\mu - \cos\eta}.$$

(1)

The metric coefficients for the coordinates are then

$$h_\mu = h_\eta = \frac{a}{\cosh\mu - \cos\eta}, \quad h_\phi = \frac{a\,\sinh\mu}{\cosh\mu - \cos\eta}.$$

(2)

In toroidal coordinates the force=free magnetic field equation, $\nabla \times \boldsymbol{B} = \alpha \boldsymbol{B}$**,** yields the following three equations

$$h_\eta B_\eta = -\frac{1}{\alpha h_\phi}\partial_\mu(h_\phi B_\phi),$$

$$h_\mu B_\mu = \frac{1}{\alpha h_\phi}\partial_\eta(h_\phi B_\phi),$$

$$\partial_\mu(h_\eta B_\eta) - \partial_\eta(h_\mu B_\mu) = \frac{\alpha h_\eta}{\sinh\mu}(h_\phi B_\phi).$$

(3)

The divergence of $\boldsymbol{B}$ is given by

$$\nabla \cdot \boldsymbol{B} = \frac{1}{h_\mu h_\eta h_\phi}[\partial_\mu(h_\eta h_\phi B_\mu) + \partial_\eta(h_\phi h_\mu B_\eta) + \partial_\phi(h_\mu h_\eta B_\phi).$$

(4)

Imposing axial symmetry ($\partial_\phi B_\phi = 0$) and the requirement that $\nabla \cdot \boldsymbol{B} = 0$ results in

$$\partial_\mu(h_\eta h_\phi B_\mu) + \partial_\eta(h_\phi h_\mu B_\eta) = 0.$$

(5)

This means that α is only a function of $h_\phi B_\phi$; that is, $\alpha = \alpha(h_\phi B_\phi)$. The force-free relation also implies that $\nabla\alpha \cdot \boldsymbol{B} = 0$. Since α is not a function of ϕ by symmetry, this implies in turn that

$$\partial_\eta\,\alpha = -\frac{B_\mu}{B_\eta}\partial_\mu\alpha.$$

(6)

Combining Eq. (6) with Eqs. (3) yields the differential equation,

$$\partial_\mu\left(\frac{1}{h_\phi}\partial_\mu(h_\phi B_\phi)\right)+\partial_\eta\left(\frac{1}{h_\phi}\partial_\eta(h_\phi B_\phi)\right)+\frac{\partial_\mu\alpha}{\alpha h_\phi}\left(\frac{B_\mu}{B_\eta}\,\partial_\eta(h_\phi B_\phi)-\partial_\mu(h_\mu B_\mu)\right)$$
$$+\frac{\alpha^2 h_\eta}{\sinh\mu}(h_\phi B_\phi)=0 \qquad (7)$$

This equation leads to an intractable equation for α, but will be simplified by imposing the boundary condition on B_μ discussed below.

Boundary Conditions

The cylindrically symmetric Lundquist solution to the force-free field equations is shown in Fig. 2. The Lundquist solution [4] is obtained by restricting α to a constant and further restricting the magnetic field to the form $\boldsymbol{B}=[0,B_\phi(r),B_z(r)]$.

The field equations will then give the solution $\boldsymbol{B}=A_0[0,J_1(\alpha r),J_0(\alpha r)]$, where J_0 and J_1 are Bessel functions and A_0 is a constant.

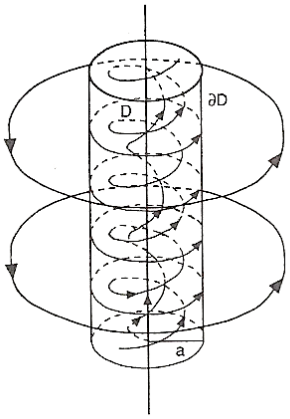

Figure 2. The Lundquist solution. The figure is drawn so that $B_z = J_0(\alpha a) = 0$ on the cylinder $r = a$.

If one chooses to apply the solution $\boldsymbol{B}=A_0[0,J_1(\alpha r),J_0(\alpha r)]$ in a cylindrical region D bounded by ∂D (as shown if Fig.2) such that $J_0(\alpha a)=0$, the solution matches smoothly to an external field given by $\boldsymbol{B}=[0,(aA_0/r)\,J_1(\alpha a),0]$ and no surface currents are required to satisfy the boundary condition.

As is the case for the cylindrically symmetric Lundquist solution, the force-free field in the interior of a torus will create an azimuthal field around the torus, but if $\nabla \cdot \boldsymbol{B} = 0$ the magnetic field normal to the surface of the torus at $\mu = \mu_0$ must vanish; i.e., $B_\mu(\mu_0) = 0$. It is this boundary condition, $B_\mu(\mu_0) = 0$, that will be used in what follows to find the magnetic field—and since it is force-free also the current—distribution on the surface of a toroid. B_μ does not necessarily vanish in the interior of the torus, but if the form of the field is restricted to the form $\boldsymbol{B} = [0, B_\eta(r), B_\phi(r)]$, then $B_\mu = 0$ on each torus given by $\mu = constant$ and the solution found applies to the interior of the torus as well.

The Equation for α on the Surface of the Torus,

The following differential equation for α follows from that of Eq. (7) combined with the assumption that B_μ vanishes everywhere.

$$\partial_\mu\left(\frac{1}{h_\phi}\partial_\mu(h_\phi B_\phi)\right) - \frac{\partial_\mu \alpha}{\alpha h_\phi}\,\partial_\mu(h_\phi B_\phi) + \frac{\alpha^2 h_\eta}{\sinh\mu}(h_\phi B_\phi) = 0 \tag{8}$$

Equation (8) has, unsurprisingly, two solutions [5]

$$\alpha = \pm\frac{1}{a}[\sqrt{(-\cos^2\eta + \cos\eta\,\cosh\mu + \cos^2\eta\,\coth^2\mu - 2\cos\eta\,\cosh\mu\,\coth^2\mu + \cosh^2\mu\,\coth^2\mu - \sinh^2\mu)}]. \tag{9}$$

When η is held constant, say in the positive equation, and α plotted as a function of μ, α grows monotonically with increasing μ. In what follows, it will be seen that the field winds around the torus and the sign of α determines the handedness of the field while the period of the twisting field is given by $|\alpha|$.

With reference to Fig. 1, henceforth $\mu = 1$ and $a = 2$ will generally be used. The plot of both solutions given by Eq. (9) for α is shown in Fig. 3.

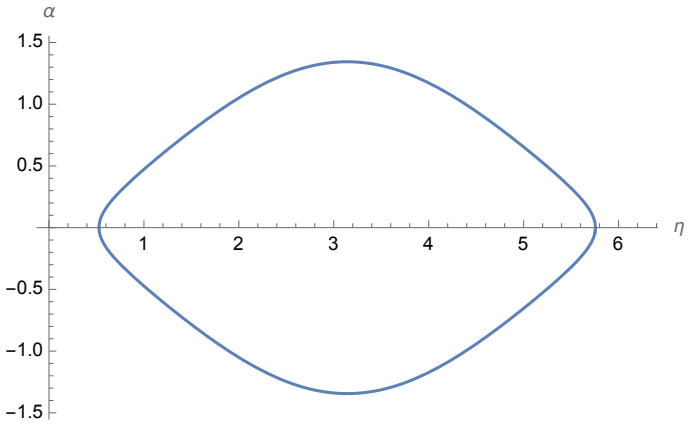

Figure 3. The plot of both solutions for α in Eq. (9) as a function of η where $0 \leq \eta \leq 2\pi$.

Figure 3 shows that the solutions for α do not cover the full range of η from $0 \leq \eta \leq 2\pi$. For $0 \leq \eta \leq 0.529$ and $5.753 \leq \eta \leq 2\pi$, α is pure imaginary so that the solutions given in Eq. (9) are not applicable. In these regions, the real part of α vanishes and since α must be a real function, the force-free relation $\nabla \times \boldsymbol{B} = \alpha \boldsymbol{B}$ implies that the field $\boldsymbol{B}$ is given by the gradient of a scalar function. It will be seen below that the transition from a force-free field to this gradient field is smooth with $\boldsymbol{B}$ always greater than zero so that the field is non-singular.

The Force-Free Field on the Torus

With $B_\mu(\mu_0) = 0$, Eqs. (3) imply that $h_\phi B_\phi = C_1$, where C_1 is a constant so that $B_\phi = C_1/h_\phi$. In Eq. (4), $\nabla \cdot \boldsymbol{B} = 0, B_\mu = 0$, and cylindrical symmetry imply that $\partial_\eta(h_\mu h_\phi B_\eta) = 0$ so that $B_\eta = C_2/h_\phi h_\mu$. Figure 4 shows B_ϕ and B_η for $C1 = 1$, $C2 = 2$, with μ =1 and a=2.

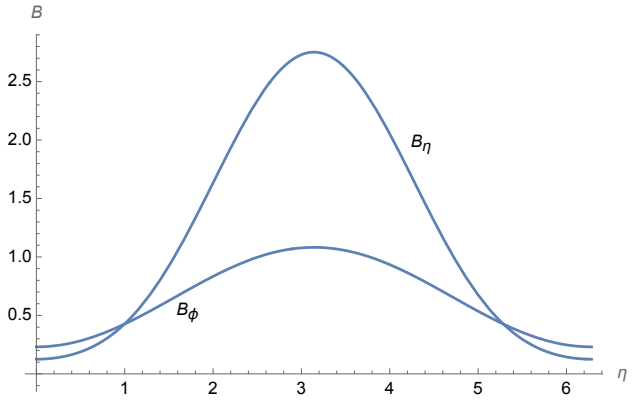

Figure 4. B_ϕ and B_η plotted for $0 \leq \eta \leq 2\pi$.

Where the curves for B_ϕ and B_η cross the magnitude of these components are equal so that the angle of their vector is at $\pi/4$ radians with respect to $\hat{\phi}$. The magnitude of the components depends on the choice of the constants C1 and C2.

Note that in the regions $0 \leq \eta \leq 0.529$ and $5.753 \leq \eta \leq 2\pi$, where α is pure imaginary there is no discontinuity in the field components and that the components B_ϕ and B_η never vanish so that the vector field they represent is not singular. Coupled with the fact that α is not constant, the field satisfies Arnold's requirements for a force-free field on a torus.

The fact that this solution has a smooth transition from a force-free magnetic field to a field given by the gradient of a scalar function in the regions $0 \leq \eta \leq 0.529$ and $5.753 \leq \eta \leq 2\pi$ is one of the most interesting features of the solution.

A vector plot of the vector $\boldsymbol{B} = (0, B_\phi, B_\eta)$ gives a better idea what the field looks like. This is shown in Fig. 5.

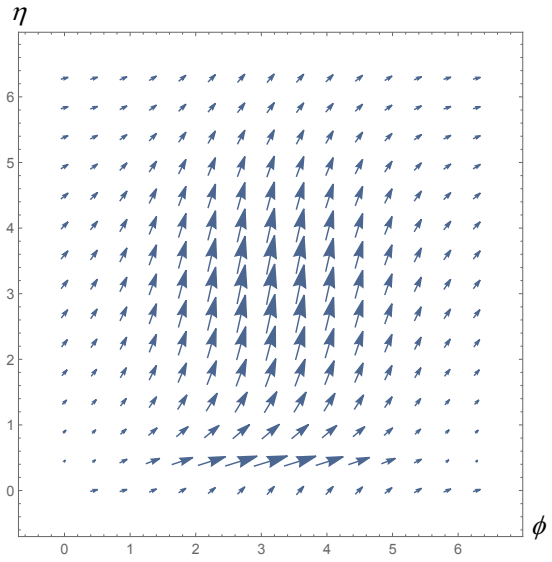

Figure 5. This is a plot of the vector field $\boldsymbol{B} = (0, B_\phi, B_\eta)$ as a function of ϕ and η. The magnitude of the field is given by the length of the arrows. For a given η the projection of the vectors on the ϕ-axis (the B_ϕ component), remains constant so that axial symmetry is preserved. The angle of the vectors along a given η with the ϕ-axis changes with ϕ, although that is somewhat difficult to see in the figure.

This field is unusual since both the pitch and magnitude change with location on the surface of the torus. This should be compared to the Lundquist solution shown in Fig. 2 and its surface at $r = a$.

Considering only the plot of Fig. 5 itself, without the "padding" around it, one can get idea of how the field looks on a torus by identifying the ϕ sides of this plot and then identifying the ends of the resulting cylinder.

Alternatively, one can use a stream plot, which loses the magnitude information. The stream plot itself is shown in Fig 6 and its mapping onto the torus in Fig. 7.

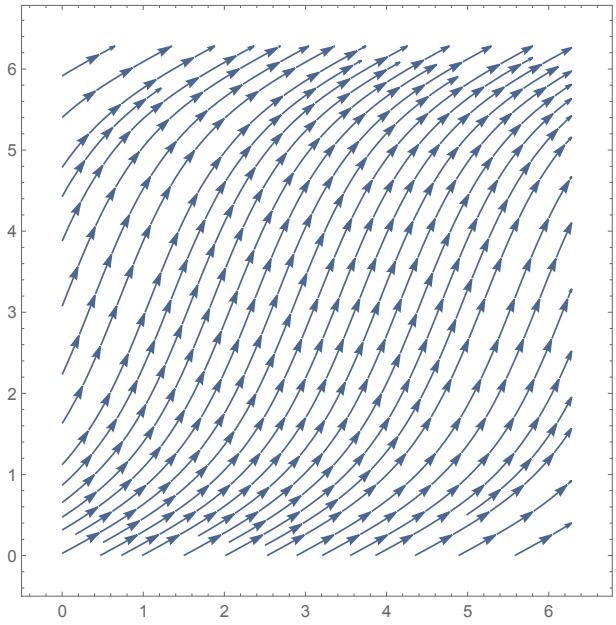

Figure 6. A stream plot of the vector field shown in Fig. 5. The magnitude information of Fig. 5 cannot be made a part of this plot.

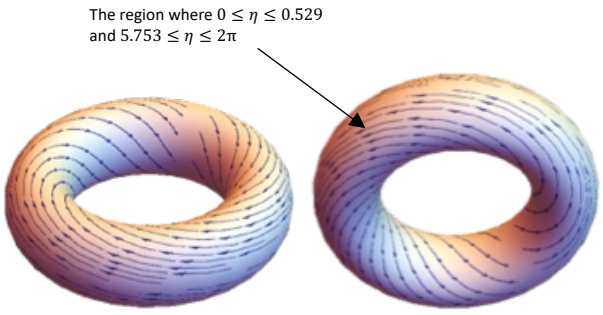

Figure 7. Two views of the stream plot of Fig. 6 mapped onto the torus. The gap seen in the first figure is an artifact of the mapping and not a discontinuity in the field. The region on the perimeter of the torus where the field becomes a gradient field is also indicated.

In producing the plots in Fig. 7 the axes and "padding" around the stream plot in Fig. 6 were remove before doing the mapping. Unfortunately, the mapping program only recognizes the removal of the axes--hence the gap seen particularly in the first figure. It is not real and only an artifact of the mapping.

REFERENCES

[1] Arnold, V.I. *Sel. Math. Sov*. **5**, 327 (1986), p.330.

[2] G. Godbillon, *Dynamic Systems on Surfaces* (Springer-Verlag, Berlin 1980), p. 181.

[3] Marsh, G.E., *Force-Free Magnetic Fields; Solutions, Topology and Applications* (World Scientific, New Jersey 1996), §3.3.

[4] Lundquist, S., *Phys. Rev.* **83**,307 (1951).

[5] Mathematica V10.1.0.0 was used to solve Eq. (5) and produce the subsequent figures.

ADDITION 2

Following the addition above add *A Force-Free Magnetic Field in Cyclidal Coordinates* from my 2023 paper, which is available at http://arxiv.org/abs/2310.17673.

INTRODUCTION

In plasma physics, where the condition for plasma equilibrium is given by $(\nabla \times \boldsymbol{B}) \times \boldsymbol{B} = \nabla p$, where *p* is the plasma pressure, the magnetic field will be force-free if $\nabla p = 0$. Force-free means that the "self-force" or Lorentz force vanishes. Force-free magnetic field configurations are difficult to find because $(\nabla \times \boldsymbol{B}) \times \boldsymbol{B} = 0$ is a nonlinear equation. The plasma β is defined as the ratio of the plasma pressure to the magnetic pressure p_m. The force-free approximation is valid for "low-beta" plasmas. Such plasmas are often found in an astrophysical context. Here it is shown that force-free fields can not only have solutions for toroids, as was shown in an earlier paper, but also for cyclides.

Dupin cyclides are those surfaces where the curvature lines are circles. The curvature lines are given by the parametric variables *u* and *v* with one or the other being equal to a constant. Of course, this is also true for tori, which—as will be discussed below—arise from setting two

of the parameters of an elliptic cyclide equal. An elliptic cyclide has a parametric representation in three-dimensional Cartesian coordinates as [1]

$$x = \frac{d(c - a\,cosu\,cosv) + b^2 cosu}{a - c\,cosu\,cosv},$$
$$y = \frac{b\,sinu(a - dcosv)}{a - c\,cosu\,cosv},$$
$$z = \frac{b\,sinv(c\,cosu - d)}{a - c\,cosu\,cosv},$$
$$0 \leq u, v < 2\pi.$$

(Eqs. 1)

Figure 1 gives an example of an elliptic cyclide and also a cutaway view of nested elliptic cyclides. The lines of curvature are given by *u* and *v* with one or the other being equal to a constant; i.e., for a constant value of *v*, *u* follows the curvature circle around the cyclide the long way and for a constant value of *u*, *v* follows the curvature circle around the cyclide the short way.

Focal conics can be seen as degenerate focal surfaces: Dupin cyclides are the only surfaces where focal surfaces collapse to a pair of curves that are focal conics. In the case of the elliptic cyclides the focal conics are an ellipse and a hyperbola. The plane of the hyperbola is orthogonal to the plane containing the ellipse and the hyperbola is the focal conic to the ellipse.

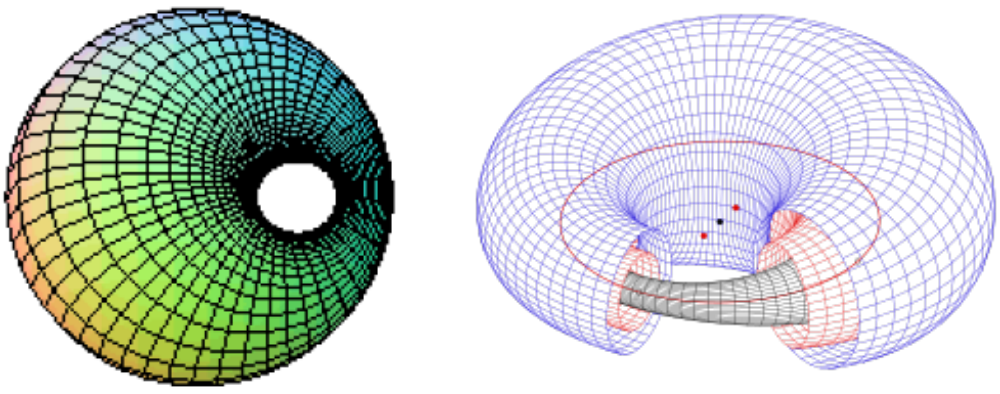

(a) (b)

Figure 1. (a) An elliptic cyclide. Note the perpendicular lines of curvature. (b) Parallel or nested surfaces of an elliptic cyclide. The parameters of the surfaces are: *a* = 1, *b* = 0.98, c = 0.199 and d, which specifies each of the cyclide surfaces, is *d* = 0.30, 0.45, and 0.60. The ellipse shown in the figure is discussed below [Source: Wikimedia Commons].

The parameters *a*, *b*, *c*, *d* in Eqs. (1) are the semi-major and semi-minor axes of the ellipse and *c* is its eccentricity. A Dupin cyclide can be considered to be a channel surface (the envelope of a one-parameter family of spheres) and *d* would be the average radius of the generating spheres. The equations of the ellipse and hyperbola are

$$\frac{x^2}{a^2}+\frac{y^2}{b^2}=1, \quad z=0,$$
$$\frac{x^2}{c^2}-\frac{z^2}{b^2}=1, \quad y=0,$$
$$0<b\le a,\ c^2=a^2-b^2.$$

Eqs. (2)

The implicit equation [1], meaning that the equation is not solved for the variables *x*, *y*, or *z*, is important for relating elliptic cyclides to tori of revolution. It is given by

$$(x^2+y^2+z^2+b^2-d^2)^2-4(ax-cd)^2-4b^2y^2=0.$$

Eq. (3)

In Eq. (3) some authors omit the factor 4 in the last term. The idea is to set *a* = *b* and show that *c* = 0 so that the ellipse becomes a circle and the hyperbola degenerates into a line so that the corresponding degenerate cyclides are tori of revolution thus showing that the torus belongs to the class of elliptic cyclides. However, Eq. (3) is very difficult to solve for *c* because the coefficients are inexact, but if one sets *a* = *b* = 1 and *d* = 0.3, one can obtain a solution by solving a corresponding exact system and "numericizing" the result. It turns out that *c* is indeed equal to zero.

THE FORCE-FREE MAGNETIC FIELD EQUATIONS IN CYCLIDAL COORDINATES

The general solution to the force-free field equations in cyclidal coordinates is a very difficult problem. The force-free field equation is $\nabla \times \boldsymbol{B} = \alpha \boldsymbol{B}$, where the expressions for the curl or divergence are non-illuminating complex functions of trigonometric functions that are very, very long. Some simplifications must be imposed. Because the divergence of the magnetic field must vanish, it is assumed here that the normal component of the magnetic field must vanish on the surface of the cyclide. Strictly speaking, a cyclide does not have cylindrical symmetry, making finding a solution almost impossible.

But, as discussed above, the lines of curvature of any Dupin cyclide are circles having the parametric coordinates *u* and *v*. To obtain a viable solution to the force-free magnetic field equations, cylindrical symmetry is assumed for each of the *u* circular coordinate lines upon which *v* is a constant. This means that B_u is constant along each *u*-circle. This is unusual because the planes containing the *u*-circles where *v* equals a constant are not parallel.

If *w* represents the coordinate normal to the cyclidal surface, the metric coefficients in cyclidal coordinates, which can be found from Eqs. (1) are:

$$
\begin{aligned}
\boldsymbol{h_u} = & \\
& \sqrt{\left(\frac{\mathbf{1}}{(\boldsymbol{a}-\boldsymbol{c}\cos(\boldsymbol{u})\cos(\boldsymbol{v}))^{\mathbf{4}}}\right.} \\
& \quad \left(\sin^2(\boldsymbol{u})\left(\boldsymbol{a}\,\boldsymbol{b}^2-\boldsymbol{d}\left(\boldsymbol{a}^2-\boldsymbol{c}^2\right)\cos(\boldsymbol{v})\right)^2+\right. \\
& \qquad \boldsymbol{b}^2\,\boldsymbol{c}^2\sin^2(\boldsymbol{u})\sin^2(\boldsymbol{v})\,(\boldsymbol{a}-\boldsymbol{d}\cos(\boldsymbol{v}))^2+ \\
& \qquad \left.\left.\boldsymbol{b}^2\,(\boldsymbol{a}-\boldsymbol{d}\cos(\boldsymbol{v}))^2\,(\boldsymbol{a}\cos(\boldsymbol{u})-\boldsymbol{c}\cos(\boldsymbol{v}))^2\right)\right), \\
\boldsymbol{h_v} = & \\
& \sqrt{\left(\frac{\mathbf{1}}{(\boldsymbol{a}-\boldsymbol{c}\cos(\boldsymbol{u})\cos(\boldsymbol{v}))^{\mathbf{4}}}\right.} \\
& \quad \left(\cos^2(\boldsymbol{u})\sin^2(\boldsymbol{v})\left(\boldsymbol{d}\left(\boldsymbol{c}^2-\boldsymbol{a}^2\right)+\boldsymbol{b}^2\,\boldsymbol{c}\cos(\boldsymbol{u})\right)^2+\right. \\
& \qquad \boldsymbol{a}^2\,\boldsymbol{b}^2\sin^2(\boldsymbol{u})\sin^2(\boldsymbol{v})\,(\boldsymbol{d}-\boldsymbol{c}\cos(\boldsymbol{u}))^2+ \\
& \qquad \left.\left.\boldsymbol{b}^2\,(\boldsymbol{d}-\boldsymbol{c}\cos(\boldsymbol{u}))^2\,(\boldsymbol{c}\cos(\boldsymbol{u})-\boldsymbol{a}\cos(\boldsymbol{v}))^2\right)\right), \\
\boldsymbol{h_w} = & \\
& \left(\left(\boldsymbol{a}^2\cos^2(\boldsymbol{u})\cos^2(\boldsymbol{v})-\mathbf{2}\,\boldsymbol{a}\,\boldsymbol{c}\cos(\boldsymbol{u})\cos(\boldsymbol{v})+\boldsymbol{b}^2\sin^2(\boldsymbol{u})\cos^2(\boldsymbol{v})+\right.\right. \\
& \qquad \left.\left.\boldsymbol{b}^2\sin^2(\boldsymbol{v})+\boldsymbol{c}^2\right)\Big/(\boldsymbol{a}-\boldsymbol{c}\cos(\boldsymbol{u})\cos(\boldsymbol{v}))^2\right).
\end{aligned}
$$

Eqs. (4)

In arbitrary curvilinear coordinates the divergence of ***B*** is given by

$$\boldsymbol{\nabla}\cdot\boldsymbol{B}=\frac{1}{\sqrt{g}}\partial_{x_i}(\sqrt{g}B^i),$$

Eq. (5)

where $g=\left|g_{ij}\right|,\ i=u,v,w.$ The calculations for the force-free fields will be greatly simplified if advantage is taken of the requirement that the normal component of the

magnetic field, B_w, must vanish on the surface of the cyclide. This allows the introduction of a flux function Φ. Equation (5) will then be satisfied if a function is introduced such that

$$\sqrt{g}B^u = \partial_v\Phi, \qquad \sqrt{g}B^v = -\partial_u\Phi.$$

Eq. (6)

A Dupin cyclide has orthogonal coordinates, and for such coordinates $g_{ij} = g^{ij} = 0, i \neq j$; the metric coefficients h_i are defined by $g_{ii} = h_i^2,\ g^{ii} = 1/h_i^2; \sqrt{g} = h_u h_v h_w$. And the physical components are then $h_i B^i$. From Eq. (6) these may be written as

$$B_u = \frac{1}{h_v h_w}\partial_v\Phi, \qquad B_v = -\frac{1}{h_u h_w}\partial_u\Phi.$$

Eqs. (7)

What remains to do in order to use this approach of making use of a flux function is to find the function itself and show that the fields of Eq. (7) are solutions of the force-free field equations. However, finding the flux function in coordinates far simpler than cyclidal coordinates can be a very difficult problem [2]. There is, however, a simpler way to find the flux function: Equations (7) imply that

$$d\Phi = h_v h_w B_u - h_u h_w B_v,$$

Eq. (8)

so that given test functions for B_u and B_v one can integrate Eq. (8) to find Φ. Finding appropriate test functions is a question of intuition. What is done here is to choose one that looks interesting when mapped onto the cyclide. Here is a simple example that will used

$$B_u = 2/h_v \; and \; B_v = 10/h_u.$$

Eqs. (9)

The flux function is then

$$\Phi = 2\int h_w dv - 10\int h_w du.$$

Eq. (10)

Given the coefficients *a*, *b*, *c*, *d*, the flux function Φ is:

$$\Phi = \frac{1}{c^2}\left(5\left(\frac{8\sqrt{2}\,a\left(a^2-b^2-c^2\right)\text{ArcTanh}\left[\frac{\sqrt{2}\,(a+c\cos[v])\tan\left[\frac{u}{2}\right]}{\sqrt{-2a^2+c^2+c^2\cos[2v]}}\right]\left(a^2-c^2\cos[2v]\right)}{\left(-2a^2+c^2+c^2\cos[2v]\right)^{3/2}}+\right.\right.$$
$$\left(-2a\left(a^2-b^2\right)c^2u\cos[v]^2+a\left(a^2-b^2\right)u\left(4a^2-c^2-c^2\cos[2v]\right)+\right.$$
$$2\left(a^2-b^2\right)cu\cos[u]\cos[v]\left(-2a^2+c^2+c^2\cos[2v]\right)+$$
$$\left.4c\left(-a^2+c^2\right)\left(-a^2+b^2+c^2\right)\cos[v]\sin[u]\right)/$$
$$\left.\left.\left((a-c\cos[u]\cos[v])\left(-2a^2+c^2+c^2\cos[2v]\right)\right)\right)-$$

$$\frac{1}{c^2}\left(\frac{8\sqrt{2}\,a\left(a^2-b^2-c^2\right)\text{ArcTanh}\left[\frac{\sqrt{2}\,(a+c\cos[u])\tan\left[\frac{v}{2}\right]}{\sqrt{-2a^2+c^2+c^2\cos[2u]}}\right]\left(a^2-c^2\cos[2u]\right)}{\left(-2a^2+c^2+c^2\cos[2u]\right)^{3/2}}+\right.$$
$$\left(-2a\left(a^2-b^2\right)c^2v\cos[u]^2+a\left(a^2-b^2\right)v\left(4a^2-c^2-c^2\cos[2u]\right)+\right.$$
$$\left(a^2-b^2\right)c^3v\cos[u]^3\cos[v]+$$
$$c\cos[u]\left(-\frac{1}{2}\left(a^2-b^2\right)v\left(8a^2-3c^2-3c^2\cos[2u]\right)\cos[v]+\right.$$
$$\left.\left.4\left(a^2-c^2\right)\left(a^2-b^2-c^2\right)\sin[v]\right)\right)/$$
$$\left.\left.\left(\left(-2a^2+c^2+c^2\cos[2u]\right)(a-c\cos[u]\cos[v])\right)\right).$$

Eq. (11)

Putting in the numerical value for the constants of a = 1, b = 0.98, c = 0.199, and d = 0.3, one can compute the flux function. The stream and vector plots of the fields in Eqs. (9) are shown below and then mapped onto the cyclide:

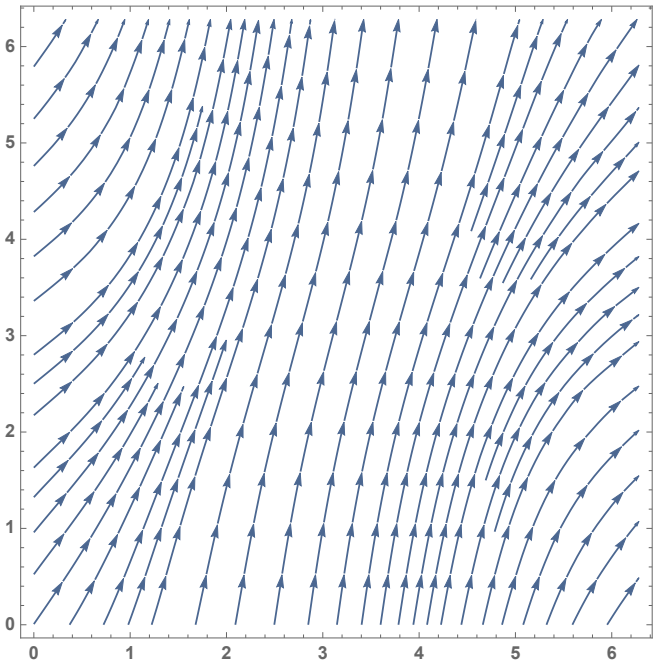

Figure 2. Stream plot of the magnetic field components given by Eqs. (9). The u-axis is along the abscissa and the v-coordinate along the ordinate.

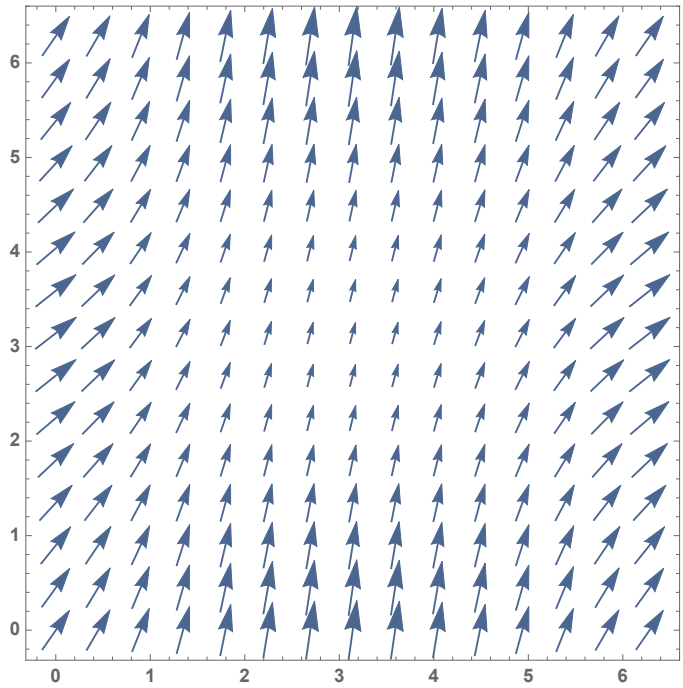

Figure 3. Vector plot of the magnetic field components given by Eqs. (9). The u-axis is again along the abscissa and the v-coordinate along the ordinate.

The stream plot mapped onto the cyclide, using the numerical values of the constants given above, is shown in Fig. 4, and the vector plot on the cyclide by Fig. 5.

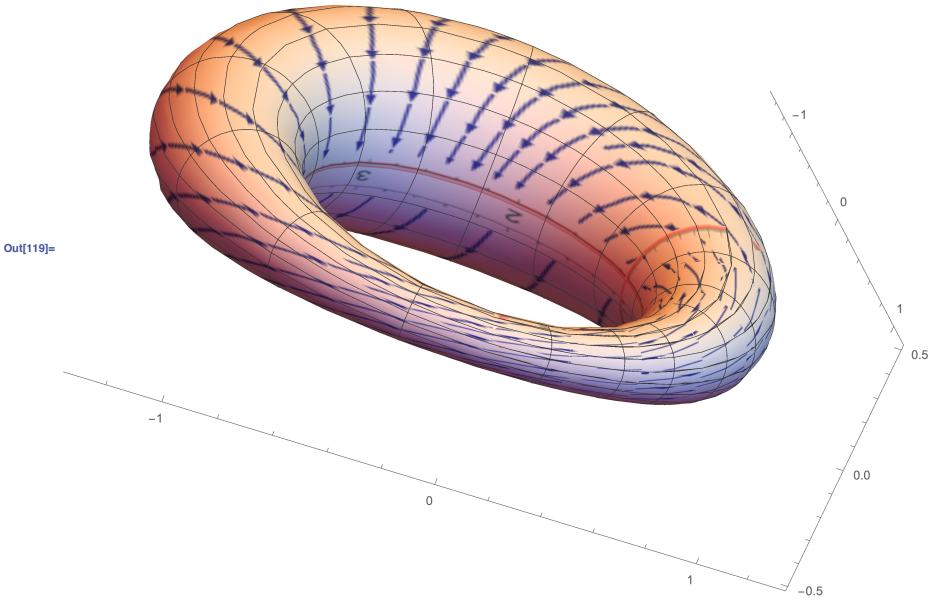

Figure 4. Stream plot of the magnetic field components specified by the flux function Φ, given by Eq. (11), mapped onto the cyclidal surface.

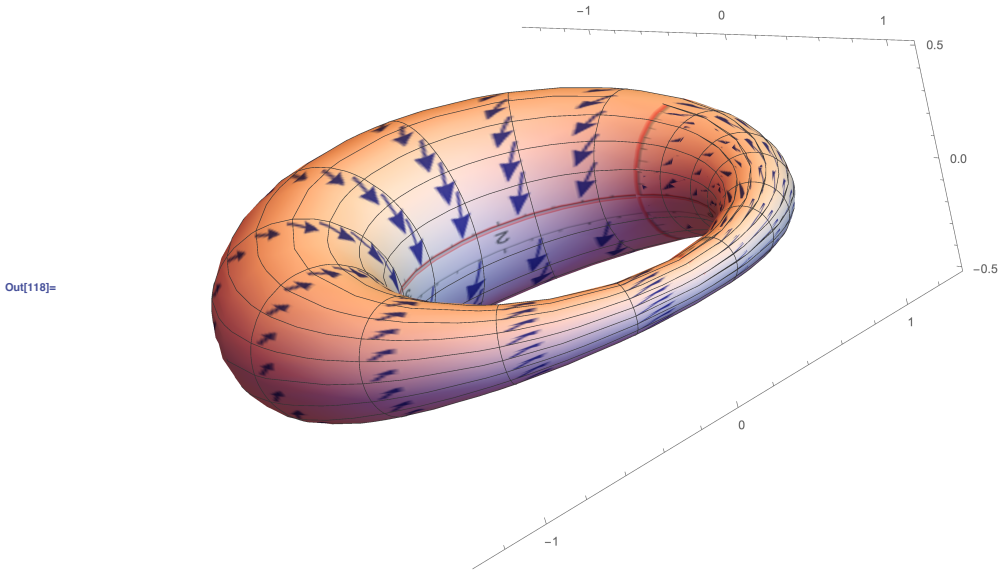

Figure 5. Vector plot of the magnetic field components specified by the flux function Φ, given by Eq. (11), mapped onto the cyclidal surface.

It remains to show that the force-free field equations are satisfied by the magnetic fields of Eqs. (9) by finding an expression for the associated function α.

The force-free field equation in 3-dimensional space is given by $\nabla \times \boldsymbol{B} = \alpha \boldsymbol{B}$; but it has been assumed here that the normal component of the magnetic field must vanish on the surface of the cyclide so that the divergence of the magnetic field vanishes. This means that the field equation must be evaluated on the surface of the cyclide and the 3-dimensional curl cannot be used.

Consequently, on the surface one must use the 2-dimensional component of the curl, also known as the circulation in another context. It is given by

$$(\nabla \times \boldsymbol{B})_w = \frac{1}{h_u h_v}(\partial_u(h_v B_v) - \partial_v(h_u B_u)).$$

Eq. (12)

The full equation for $(\nabla \times \boldsymbol{B})_w$ with the meanings of the symbols inserted is very long and there is little if any insight to be gained. It is available in the original paper.

The force-free field equation to be solved for the function α is then

$$\frac{1}{h_u h_v}(\partial_u(h_v B_v) - \partial_v(h_u B_u)) = \alpha(B_u + B_v).$$

Eq. (13)

The solution for α is again very long, offering no insight, and it is available in the original paper.

Figures 6(a) and 6(b) show 3-dimensional plots of the function α. The cross sections at $u = 0$ and $u = 2\pi$ match since they represent the same cross section on the cyclide and the same is true for $v = 0$ and $v = 2\pi$. Note the changes in sign of the function α. In the regions where α is zero, the curl vanishes and the magnetic field is the gradient of a scalar function.

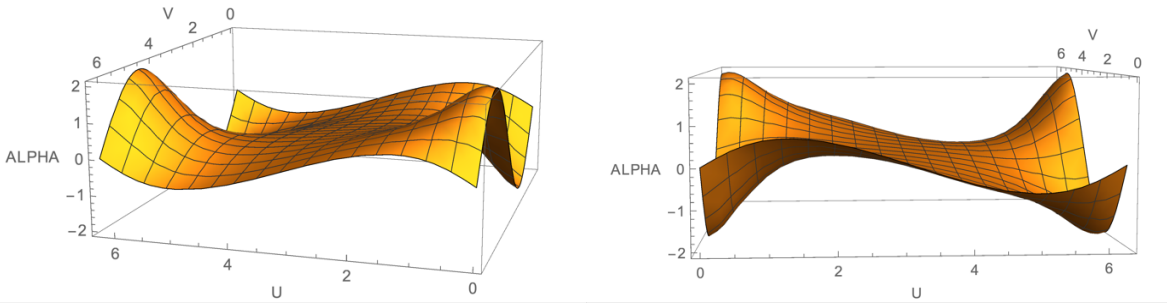

Figure 6. 3-dimensional plots of the solution for the function α of Eq. (13). The variables *u* and *v* are shown as capitals in the figures to make them easier to read.

The solution given above is then an example of a solution to the problem of finding a force-free magnetic field on the surface of a cyclide.

CYCLIDE TO TOROID

As mentioned in the Introduction, the torus belongs to the class of elliptic cyclides. By setting the coefficients $a = b$ and $c = 0$, the flux function approach to finding solutions used above should yield a solution on a torus. It is shown in this section that that is indeed true. To make comparison easier the values of the constants are now chosen to be $a = b = 1$, $c = 0$, and $d = 0.3$. With these values the metric coefficients of Eqs. (4) become

$$h_u = \sqrt{\cos^2(u)(1 - 0.3\cos(v))^2 + \sin^2(u)(1 - 0.3\cos(v))^2},$$
$$h_v = \sqrt{0.09\sin^2(u)\sin^2(v) + 0.09\cos^2(u)\sin^2(v) + 0.09\cos^2(v)},$$
$$h_w = \cos^2(u)\cos^2(v) + \sin^2(u)\cos^2(v) + \sin^2(v).$$

Eqs. (14)

And, using the same magnet field components as used above, we obtain for the flux function the simple result $\Phi = -10u + 2v$.

The stream and vector plots for the degenerate cyclide are shown in Fig. (7)

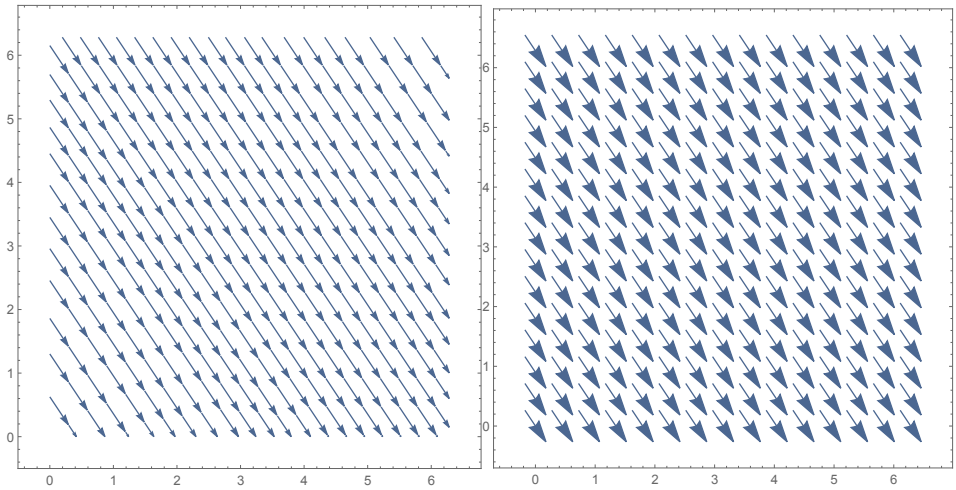

Figure 7. Stream and vector plots of the magnetic field components given by Eqs. (9), but in this case for the degenerate cyclide. The *u*-axis is again along the abscissa and the *v*-coordinate along the ordinate.

When the stream and vector plots are mapped onto the degenerate cyclide, as shown in Figs. (8), it is obvious that the degenerate cyclide is indeed a torus.

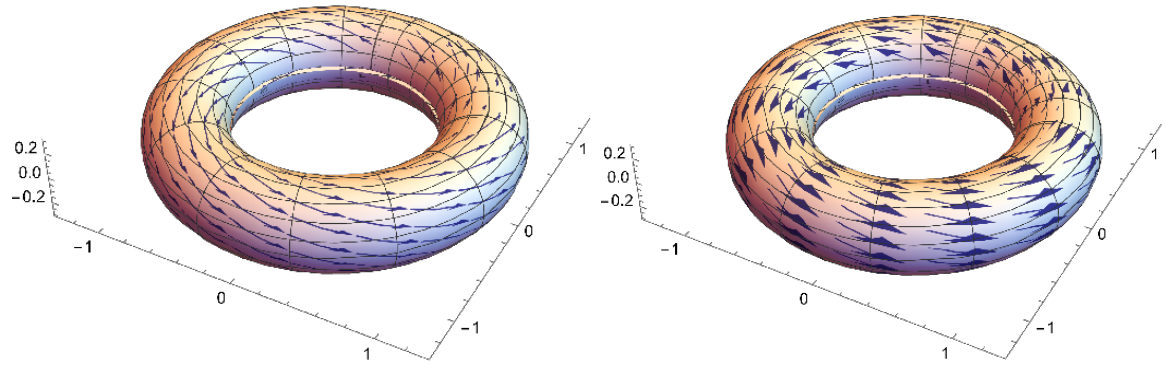

Figure 8. Stream and vector plots of the magnetic field components given by Eqs. (9), mapped onto the degenerate cyclide.

The plot of the magnetic field mapped on the torus is different and much less complex than that found in Reference [3]. The flux function approach can be used to find many other force-free magnetic field solutions for the torus.

In order to show that this example is a solution to the force-free field equations, it must be demonstrated that there exists an appropriate function α. Solving for the function α using Eq. (13) results in

$$\alpha = \left(1.` \left(-\left(\left(1.` \left(0.6` \cos^2(u) \sin(v) (1.` - 0.3` \cos(v)) + 0.6` \sin^2(u) \sin(v) (1.` - 0.3` \cos(v))\right)\right) \Big/ \left(\sqrt{0.09` \sin^2(u) \sin^2(v) + 0.09` \cos^2(u) \sin^2(v) + 0.09` \cos^2(v)} \sqrt{\cos^2(u) (1.` - 0.3` \cos(v))^2 + \sin^2(u) (1.` - 0.3` \cos(v))^2}\right)\right) + \left(\left(0.18` \cos^2(u) \sin(v) \cos(v) + 0.18` \sin^2(u) \sin(v) \cos(v) - 0.18` \sin(v) \cos(v)\right) \sqrt{\cos^2(u) (1.` - 0.3` \cos(v))^2 + \sin^2(u) (1.` - 0.3` \cos(v))^2}\right) \Big/ \left(0.09` \sin^2(u) \sin^2(v) + 0.09` \cos^2(u) \sin^2(v) + 0.09` \cos^2(v)\right)^{3/2} + 0.`\right)\right) \Big/ \left(\sqrt{0.09` \sin^2(u) \sin^2(v) + 0.09` \cos^2(u) \sin^2(v) + 0.09` \cos^2(v)} \left(\frac{2.`}{\sqrt{0.09` \sin^2(u) \sin^2(v) + 0.09` \cos^2(u) \sin^2(v) + 0.09` \cos^2(v)}} - \frac{10.`}{\cos^2(u) \cos^2(v) + \sin^2(u) \cos^2(v) + \sin^2(v)}\right) \sqrt{\cos^2(u) (1.` - 0.3` \cos(v))^2 + \sin^2(u) (1.` - 0.3` \cos(v))^2}\right)$$

Eq. (15)

Here is a 3-dimensional plot of the function α

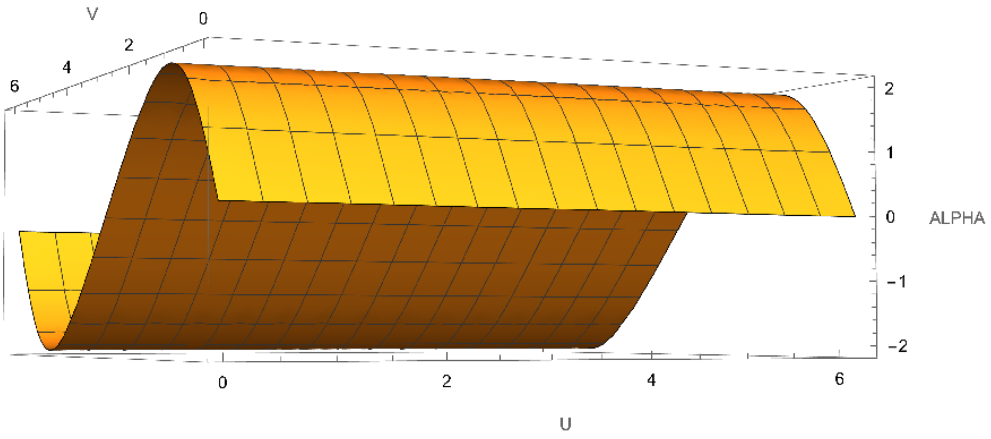

Figure 9. A 3-dimensional plot of the function α for the degenerate cyclide/torus.

The cross sections at $u = 0$ and $u = 2\pi$ match since they represent the same cross section on the torus and the same is true for $v = 0$ and $v = 2\pi$. Note the changes in sign of the function α. Where α is zero, for the degenerate cyclide/torus at *v* = 0, π, and 2π, the curl vanishes and the magnetic field is the gradient of a scalar function.

SUMMARY

Recently, the problem of finding force-free magnetic fields on a torus has been solved [2], and since the torus can be viewed as a degenerate cyclide the question naturally arises as to whether the more general problem of finding a force-free magnetic field on the surface of a cyclide can be solved for a Dupin cyclide. The torus has cylindrical symmetry which greatly simplifies the problem, but this is not the case for a cyclide. However, the lines of curvature of any Dupin cyclide are circles, allowing the introduction of a limited form of cylindrical symmetry for each of the *u* circular coordinate lines, upon which *v* is a constant. This results in a greatly simplified problem for finding a solution for a magnetic field on the cyclide, but it should be remembered that the planes containing the *u*-circles where v is constant are not parallel.

If the magnetic field is independent of one coordinate, chosen above to be the normal to the surface of the cyclide, the divergence of the magnetic field will vanish if a flux function —see Eq. (6)—is introduced. Since the coordinates introduced for the cyclide are orthogonal, the components of the magnetic field may be written as in Eq. (7). By using test functions for B_u

and B_v one can find Φ. The previous section explains the choice of the simple test functions specified in Eqs. (9).

Since it was assumed that the normal component of the magnetic field vanishes on the surface of the cyclide so as to have the divergence of the magnetic field vanish, the 3-dimensional form of the curl cannot be used in the force-free field equation. Instead, one must use the 2-dimensional component of the curl to obtain Eq. (13) which is then solved for the function α. Figure (6) shows that this function has negative values for some regions on the surface of the cyclide. In the regions where α is zero, the curl vanishes and the magnetic field is the gradient of a scalar function.

REFERENCES

[1] General introductions to cyclides and their properties: https://en.wikipedia.org/wiki/Dupin_cyclide; https://mathcurve.com/surfaces.gb/cycliddedupin/cyclidededupin.shtml
[2] G.E. Marsh, *Force-Free Magnetic Fields* (World Scientific Publishing Co. Ltd., New Jersey 1996), Sect. 3.2.1.
[3] G.E. Marsh, "A Force-Free Magnetic Field Solution in Toroidal Coordinates", *Physics of Plasmas* **30**, 5 (2023).

ADDITION 3

P. 117. In the Applications chapter after Section 6.2 add "The chiral anomaly, Dirac and Weyl semimetals, and force-free magnetic fields" from my 2017 paper in the Canadian Journal of Physics available at http://arxiv.org/abs/1605.09214.

INTRODUCTION

A 2015 paper by Xiong, et al. [1] reported that the chiral anomaly, usually considered a purely quantum mechanical phenomenon, can be seen in the Dirac semimetal Na_3Bi. The phenomenon appears in this material when the applied electric field and magnetic fields are parallel. Because new macroscopic quantum effects are rare it is important to explore the implications of this observation.

Some terminology and basics:

When the mass is set equal to zero in the Dirac equation it decouples into two equations known as the Weyl equations that have two component spinors as solutions; these have chiralities of $\chi = \pm 1$. Now define the Hamiltonian of the Dirac semimetal $H(\boldsymbol{k})$ in terms of the

spinor basis {I, σ_1, σ_2, σ_3}. If there is a $\boldsymbol{k}_0$ such that the Hamiltonian satisfies $H(\boldsymbol{k}_0) = 0$, in the vicinity of $\boldsymbol{k}_0$ the continuity of Hamiltonian implies that it can be written as $H(\boldsymbol{k}) = \boldsymbol{h}(\boldsymbol{k}) \cdot \boldsymbol{\sigma}$. If h_i are the components of $\boldsymbol{h}$, the band structure of the Hamiltonian, $E_{\pm}(\boldsymbol{k}) = \pm\sqrt{h_1^2 + h_2^2 + h_3^2}$, is called the Dirac cone, and if $\boldsymbol{h}(\boldsymbol{k})$ is a linear function of $\boldsymbol{k}$, the cone in h-space also forms a cone in k-space. An example of a Dirac cone is shown in Fig. 1(a).

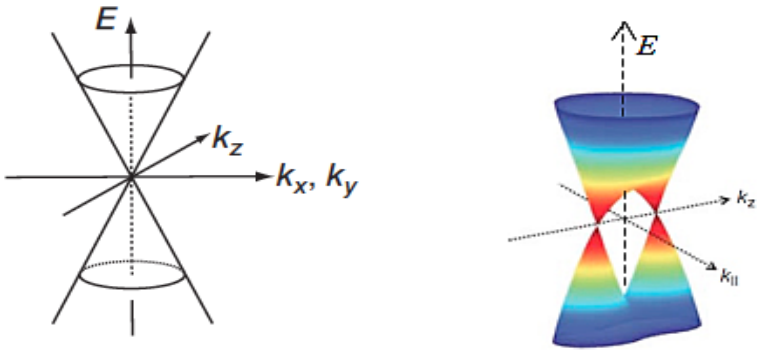

(a) (b)

Figure 1. (a) A Dirac cone. The origin is said to have a Dirac node, and the Fermi level is located where the apexes meet. The upper cone represents the conduction band and the lower the valence band. (b) When a magnetic field is applied to a Dirac semimetal it breaks the symmetry of the crystal and causes a Dirac node to split into two chiral Weyl nodes.

The Dirac cone illustrated in Fig. 1(a) corresponds to a Dirac semimetal because there is no gap between the two cones, which would become hyperbolae when a gap is present. A normal insulator has a gap and a three-dimensional topological insulator is characterized by the bulk of the material having a gap while the surface does not.

A Dirac semimetal, such as Na_3Bi, is a three-dimensional system with a Dirac cone having a double degeneracy at the Fermi energy; a Weyl semimetal has its valence and conduction bands touching each other at isolated points, around which the band structure forms non-degenerate three dimensional Dirac cones. The apexes of the Dirac cones are called Weyl nodes. Low energy quasiparticle excitations in Weyl semimetals give the first example of the appearance of massless Weyl fermions in nature.

Figure 1(b) shows the band structure of a Dirac semimetal when a strong magnetic field is applied. If there is no electric field present, chirality is preserved at the two nodes. If, however, an electric field is applied charge will flow between the nodes, and the chiral anomaly will not vanish. The charge transfer rate depends on the chirality χ (see Eq. (3.2) below). The standard textbooks on topological insulators expand on these definitions and on the topological nature of Weyl nodes and their relation to Berry curvature [2,3].

The first section below explains some aspects of the chiral anomaly and the second explains the connection with force-free magnetic fields and their relevance to the chiral anomaly observed in the semimetal Na_3Bi. The third section looks at the relaxation of such fields in a medium with a non-zero resistivity.

1. Chiral Anomaly

In classical physics there is said to be a symmetry when the action $S(\psi)$ is invariant under the transformation $\psi \rightarrow \psi + \delta\psi$, while in quantum mechanics the path integral $\int D\Psi\, e^{iS(\Psi)}$ must be invariant for a symmetry to be present. The transformation from classical to quantum mechanics does not always retain a given symmetry. Otherwise said: Symmetries in terms of classical, commuting variables may not be retained when expressed in terms on non-commuting quantum variables. Such a symmetry is said to have a "quantum symmetry anomaly".

The quantum symmetry anomaly of interest here is the axial anomaly, which violates the conservation of axial current. The non-conservation of chirality was discovered in the late 1960s by Adler [4], and Bell and Jackiw, [5]. There is a detailed discussion of the origins of the phenomenon in the textbook by Zee [6], and a very clear explication relevant to this work has been given by Jackiw [7].

The axial vector current is defined as $J_5^\mu = \psi^\dagger \gamma^0 \gamma^\mu \gamma^5 \psi$. For massless fermions, J_5^μ satisfies the continuity equation $\partial_{x^\mu} J_5^\mu = 0$. Now define $P_\pm = \frac{1}{2}(I \pm \gamma^5)$ and $\psi_\pm = P_\pm \psi$ so that $\gamma^5 \psi_\pm = \pm \psi_\pm$; then if ψ is a classical or quantum field operator the transformation

$$\psi \to e^{i\gamma^5\theta}, \quad \psi_\pm \to e^{\pm i\theta}\psi_\pm$$

(1.1)

is a map between different solutions of $i\gamma^\mu \partial_{x^\mu}\psi_\pm = 0$. If one now couples this equation to an external gauge field A_μ,

$$i\gamma^\mu(\partial_{x^\mu} + iA_\mu(x))\psi(x) = 0,$$

(1.2)

then for a single Fermi field coupling to A_μ the axial vector current J_5^μ obeys the anomalous continuity equation

$$\partial_{x^\mu} J_5^\mu = \frac{1}{8\pi^2} * F^{\mu\nu}(x) F_{\mu\nu}(x),$$

(1.3)

where $*F^{\mu\nu} = \frac{1}{2}\epsilon^{\mu\nu\alpha\beta}F_{\alpha\beta}$ is the dual of the field tensor $F_{\mu\nu}(x) = \partial_{x^\mu}A_\nu(x) - \partial_{x^\nu}A_\mu(x)$. For non-Abelian fields, $A_\mu = \sum_\alpha A_\mu^{\ \alpha} T_\alpha$ and the T_α are anti-Hermitian matrices satisfying the Lie algebra commutators with structure constants $f_{ab}^{\ c}$; i.e., $[T_a, T_b] = \sum_c f_{ab}^{\ c} T_c$. Note that the structure constants, $f_{ab}^{\ c}$, are normalized by $trT_aT_b = -\delta_{ab}/2$. For non-Abelian fields, Eq. (1.3) becomes

$$\partial_{x^\mu} J_5^\mu = \frac{1}{8\pi^2}\, tr * F^{\mu\nu}(x) F_{\mu\nu}(x).$$

(1.4)

The chiral anomaly in quantum field theory comes from two triangle Feynman diagrams associated with the decay of the π^0 particle [6].

If A_μ corresponds to the electromagnetic four potential, then Eq. (1.3) becomes

$$\partial_{x^\mu} J_5^\mu = \frac{1}{4\pi^2}\boldsymbol{E}\cdot\boldsymbol{B}.$$

(1.5)

It is this form of the anomaly that is responsible for the observations of Xiong, et al. when the electric and magnetic fields in Na_3Bi have collinear components. Note that the anomaly vanishes when the electric and magnetic fields are perpendicular; its non- vanishing depends on the component of ***B*** parallel to ***E***. If the medium cannot sustain a Lorentz force the fields must be either perpendicular or parallel. It is the parallel case that is of interest here. The insight that the chiral anomaly should appear in crystals is due to Nielsen and Ninomiya [8]. For a topical review of the electromagnetic response of Weyl semimetals see Burkov [9].

2. Chiral Anomaly and Force-Free Magnetic Fields

This section gives a short introduction to force-free magnetic fields where the current is parallel to the magnetic field, implying that the Lorentz force vanishes. In the experiment by Xiong, et al. [10], the same condition, that the current produced by an applied electric field be parallel to the magnetic field, is also required for the non-vanishing of the chiral anomaly. The origin of the current [11] is the ***E***-field parallel to ***B***, which breaks chiral symmetry and results in an axial current.

In the Dirac semimetal Na_3Bi the effect of the anomaly was observed when the applied electric field and magnetic field were aligned. Xiong, et al. suggested that the large negative magnetoresistance observed implied a long relaxation time for the current. Since the non-vanishing of the anomaly depends only on $\boldsymbol{E} \parallel \boldsymbol{B}$ not vanishing, the configuration of the field responsible for the anomaly interior to the Na_3Bi crystal is likely to be force-free. This is because the current associated with ***E*** is parallel to ***B***, and this current is itself a source for an azimuthal magnetic field that combines with the longitudinal magnetic field applied to the Na_3Bi to twist the flux. It is force-free because the current associated with ***E*** is parallel to the twisted field.

It will be seen below that force-free fields have a helicity associated with them that is related to the energy stored in the field. This opens up the possibility that the decay of such fields may explain the long axial current relaxation time in Dirac and Weyl semimetals without invoking quantum mechanical processes.

Fields with $\boldsymbol{E} \parallel \boldsymbol{B}$ are closely related to the force-free magnetic field equations $\nabla \times \boldsymbol{B} = \alpha \boldsymbol{B}$ with constant α [11]. In the experiment of Xiong, et al. [10], the applied electric field produces a current so that, because it is only the component of the electric field parallel to the applied magnetic field that yields a non-zero chiral anomaly, this current is parallel to the applied magnetic field. This means that the field is force-free. As a consequence, since the electric field corresponds to a current, $\boldsymbol{E} \parallel \boldsymbol{B}$ means that ***E*** = β ***B***, where β is a scalar function. If β is assumed to be a constant, Maxwell's equations can be used to show that $\beta = \pm i$, so there

are no real solutions. If β is assumed to only be a function of time, $\boldsymbol{E} = \beta \boldsymbol{B}$ and Maxwell's equations show that

$$\nabla \times \boldsymbol{B} = \frac{\dot{\beta}}{\beta^2 + 1} \boldsymbol{B}$$

(2.1)

This equation tells us is that if $\boldsymbol{E} = \beta(t)\, \boldsymbol{B}$, then $\boldsymbol{B}$ must satisfy the force-free field equation. The function $\dot{\beta}(\beta^2 + 1)^{-1}$ in Eq. (2.1) is actually a constant, call it α, as is shown in Appendix 1 of [11]; and this restricts the form of β to

$$\beta = i \frac{Be^{-i\alpha t} - Ae^{i\alpha t}}{Be^{-i\alpha t} + Ae^{i\alpha t}}.$$

(2.2)

If *A* or *B* vanishes, $\beta = \pm i$ so that there are no real solutions; If $A = \pm B$, then $\beta = \tan \alpha t$ or $\beta = \cot \alpha t$ respectively. Equation (2.1) can then be written as

$$\nabla \times \boldsymbol{B}(\boldsymbol{r}) = \alpha \boldsymbol{B}(\boldsymbol{r}).$$

(2.3)

Thus, any magnetostatic solution to the force-free field equations can be used to construct a solution to Maxwell's equations with $\boldsymbol{E}$ parallel to $\boldsymbol{B}$. This is true in free space (where the solutions are standing waves, which have a vanishing Poynting vector) or when $\boldsymbol{E}$ generates an electric current parallel to an external magnetic field as in the experiment of Xiong, et al. [10].

3. The Chiral Anomaly and Current Relaxation Lifetime

The long axial current relaxation time in Dirac and Weyl semimetals is poorly understood and is thought to be due to near conservation of chiral charge. Burkov [12] found that there is a coupling between the chiral and total charge density, but this leads to a large negative magnetoresistance only when the chiral charge density is a nearly conserved quantity with a long relaxation time.

Consider the form of the chiral anomaly given by Eq. (1.5). Using $\boldsymbol{E} = -\partial t \boldsymbol{A}$ and integrating over both space and time gives the helicity

$$\mathcal{H} = -\int d^3x (\boldsymbol{A} \cdot \boldsymbol{B}).$$

(3.1)

The integral on the right-hand side is the helicity of the field, $\boldsymbol{A}\cdot\boldsymbol{B}$ being the helicity density. It plays an important role in the relaxation of magnetic fields. Because helicity is a topological invariant there are conditions under which it is conserved, but here, as will be seen below, the chiral anomaly provides a mechanism for the decay of helicity that may help explain the long current relaxation time.

Fukushima, et al. [13] have shown that a "chirality imbalance" in systems with charged chiral fermions will generate an electric current in an external magnetic field; they call this the "Chiral Magnetic Effect". Because this current also acts as a source for a magnetic field, the current flowing along the magnetic field will twist the magnetic flux and induce helicity into the field. Xiong, et al. [1] have demonstrated the converse where an applied electric current causes a charge to flow from one chiral node to another of opposite chirality. That is, application of $\boldsymbol{E}\parallel\boldsymbol{B}$ causes a charge "pumping" rate *W* between the two chiral Weyl nodes

$$W=\chi\frac{e^3}{4\pi^2\hbar^2}\boldsymbol{E}\cdot\boldsymbol{B},$$

(3.2)

where $\chi=\pm1$ indicates the chirality. The "chiral imbalance" referred to above can be found by defining the number densities $\boldsymbol{n}_{L,R}=\frac{1}{2V}\int d^3x\,\psi^\dagger(1\pm\gamma^5)\psi$, where *V* is the volume and n_L corresponds to the minus sign and n_R to the plus. By integrating the total axial vector current J_5^μ over space and time one can then obtain the difference in left and right chiral particles; i.e.,

$$\boldsymbol{n}_L-\boldsymbol{n}_R=\int d^4x(\partial_\mu J_5^\mu)=\frac{1}{4\pi^2}\int d^4x(\boldsymbol{E}\cdot\boldsymbol{B}).$$

(3.3)

The integrand of the integral on the right-hand side of this equation is the chiral anomaly given by Eq. (1.5). Now differentiating Eq. (3.3) with respect to time gives

$$\frac{d}{dt}(\boldsymbol{n}_L-\boldsymbol{n}_R)=\frac{1}{4\pi^2}\int d^3x(\boldsymbol{E}\cdot\boldsymbol{B}).$$

(3.4)

Note that the integration is now over a 3-volume. If one now assumes the scalar potential vanishes and substitutes $\boldsymbol{E}=-\partial_t\boldsymbol{A}$ into Eq. (3.4), and then integrates with respect to time, $(\boldsymbol{n}_L-\boldsymbol{n}_R)$ may be expressed in terms of the helicity

$$\boldsymbol{n}_L - \boldsymbol{n}_R = -\frac{1}{4\pi^2}\int d^3x\,(\boldsymbol{A}\cdot\boldsymbol{B}) = -\frac{1}{4\pi^2}\mathcal{H}.$$

(3.5)

As a result, Eq. (3.4) can be written as

$$\frac{d}{dt}(\boldsymbol{n}_L - \boldsymbol{n}_R) = -\frac{1}{4\pi^2}\frac{d\mathcal{H}}{dt}.$$

(3.6)

A similar expression is readily derivable from the force-free field equation $\nabla\times\boldsymbol{B} = \alpha\boldsymbol{B}$, where α is again a constant. The magnetic field energy *E* due to currents ***J*** in a volume *V* is given by

$$E = \tfrac{1}{2}\int_V \boldsymbol{J}\cdot\boldsymbol{A}dV.$$

(3.7)

By taking the dot product of ***A*** with the force-free field equations and using Eq. (3.7) one obtains

$$E = \tfrac{1}{2}\alpha\int_V \boldsymbol{A}\cdot\boldsymbol{B}dV = \tfrac{1}{2}\alpha\mathcal{H}.$$

(3.8)

Now taking the derivative with respect to time and identifying $d\mathcal{H}/dt$ with the same quantity in Eq. (3.6) gives

$$\frac{d}{dt}(\boldsymbol{n}_L - \boldsymbol{n}_R) = -\frac{1}{2\pi^2\alpha}\frac{dE}{dt}.$$

(3.9)

Thus, for force-free magnetic fields, the change in the difference of the number of left and right-handed chiral particles can be related to the change in energy.

The mechanism by which the chiral anomaly allows the decay of helicity can be found by taking the time derivative of the helicity density and expanding $\partial_t(\boldsymbol{A}\cdot\boldsymbol{B})$. Using the homogeneous Maxwell equations, one can then derive the expression

$$\partial_t(\boldsymbol{A}\cdot\boldsymbol{B}) + \nabla\cdot(\boldsymbol{\Phi}\boldsymbol{B} + \boldsymbol{A}\times\boldsymbol{E}) = -2\boldsymbol{E}\cdot\boldsymbol{B}.$$

(3.10)

This is a continuity equation where $\boldsymbol{A}\cdot\boldsymbol{B}$ is the helicity density, $(\Phi\boldsymbol{B}+\boldsymbol{A}\times\boldsymbol{E})$ is the helicity current (the flux of helicity), and $-2\boldsymbol{E}\cdot\boldsymbol{B}$ is a helicity "sink". The latter can be seen to make sense by writing the integral form of Eq. (3.10):

$$\partial_t \int_V \boldsymbol{A}\cdot\boldsymbol{B}\, dV + \int_V \nabla\cdot(\Phi\boldsymbol{B}+\boldsymbol{A}\times\boldsymbol{E})\, dV = -2\int_V \boldsymbol{E}\cdot\boldsymbol{B}\, dV. \tag{3.11}$$

The integral on the right-hand side of this equation represents the resistive decay of helicity ($\boldsymbol{E}=\eta\vec{j}$ where η is the resistivity and $\vec{j}$ is the current per unit area). The rate of relaxation is determined by η. The integrand is proportional to the chiral anomaly of Eq. (1.5).

Summary

After discussion of some aspects of the chiral anomaly and its form when $F_{\mu\nu}$ is the electromagnetic field tensor, it was shown that in a conducting medium such as Na_3Bi when $\boldsymbol{E}\parallel\boldsymbol{B}$ the field must take the form of a force-free magnetic field. It was then shown that the current relaxation time in such media will depend on the decay of helicity, which in turn depends on the chiral anomaly and the resistivity of the medium. It is likely that this mechanism has some bearing on the long axial current relaxation time in Dirac and Weyl semimetals.

REFERENCES

[1] J. Xiong, et al., Science **350**, 413 (2015).
[2] Shun-Qing Shen, Topological Insusators (Springer-Verlag, Berlin 2012).
[3] F. Ortman, S. Roche, and S.O. Valenzuela, Eds. Topological Insulators: Fundamental and Perspectives (Wiley-VCH Verlag GmbH & Co. KGaA 2015).
[4] S. L. Adler, Phys. Rev. **177**, 2426 (1969).
[5] J. S. Bell and R. W. Jackiw, Nuov. Cim. A**60**, 4 (1969).
[6] A. Zee, Quantum Field Theory in a Nutshell (Princeton University Press Princeton, 2010), Section IV.7.
[7] R. W. Jackiw, Int. J. Mod. Phys. A **25.4,** 659 (2010).
[8] H. B. Nielsen and M. Ninomiya, Phys. Lett. B **130**, 389 (1983).
[9] A. A. Burkov, J. Phys: Condens. Matte*r* **27**, 113201 (2015), [arXiv: 1502.07609].
[10] J. Xiong, et al., [arXiv:1503.08179] (2015).
[11] G. E. Marsh, Force-Free Magnetic Fields: Solutions, Topology and Applications (World Scientific Publishing Co. Pte. Ltd. Singapore 1996).
[12] A. A. Burkov, Phys. Rev. *B* **91**, 245157 (2015), (arXiv:1505.01849v2 [cond-mat.mes-hall]).
[13] K. Fukushima, D.I. Kharzeev, and H.H. Warringa, arXiv:0808.3382v1 [hep-ph] (2008).